Solvent effects in the formation of hybrid materials based on titanium alkoxide-polysiloxane precursors

Sorin Ivanovici,[a] Christoph Rill,[a] Thomas Koch,[b] Michael Puchberger[a] and Guido Kickelbick*[a]

Received (in Montpellier, France) 7th January 2008, Accepted 5th February 2008
First published as an Advance Article on the web 10th March 2008
DOI: 10.1039/b800161h

Hybrid TiO_2-polysiloxane nanoparticles as well as hybrid TiO_2-polysiloxane gels were prepared and characterized applying solvent-induced aggregation effects of titanium alkoxide-modified polysiloxane block copolymers. The functionalized polymers were prepared by the covalent attachment of coordination sites that allow the binding to metal alkoxides ($M(OR)_4$; M = Ti; R = ethyl, butyl, isopropyl). Composition and structure of the hybrid polymers were investigated by NMR and FT-IR spectroscopy. In a second step the metal-alkoxide functionalities were hydrolyzed to form the respective metal oxides. Depending on the solvent in which the hydrolysis took place, hybrid nanoparticles or gels were obtained as a result of the different compatibility of the polysiloxane blocks towards the polarity of the solvents. The formed materials were investigated by NMR, FT-IR, atomic force microscopy (AFM), electron microscopy, and dynamic light scattering (DLS).

Introduction

In recent years hybrid inorganic–organic materials composed of metal oxides and polymers gained a lot of attention due to their unique properties arising from both components.[1] Hybrid materials are normally divided in two classes: class I are those that show weak interactions between the two phases (van der Waals, hydrogen bonding or weak electrostatic interactions) while materials of class II show strong chemical interactions between the components.[2] One common way to reinforce polymers and produce hybrid materials is the simple blending with nanoparticles, resulting in so called class I nanocomposite materials.[3] In such a way various nanocomposites could be obtained which have applications as thermoresistent materials, photovoltaic materials, biomaterials or drug delivery systems and biocomposites for orthopaedic surgery.[4,5] TiO_2 nanomaterials became interesting in the last years due to their unique properties with regard to their high refractive index, UV-absorption or photocatalytic properties.[6–8] Novel composite materials with both bioactivity and photoreactivity were prepared by mixing TiO_2 anatase particles with a silicone sheet as the polymer substrate.[9] Nanocomposites resulting from the incorporation of nanoparticles in polymers present the advantage that the inorganic fillers have a well-defined, previously designed morphology. One of the major problems of mixing inorganic preformed nanoparticles with polymers is the fact that aggregation of the particles due to their high surface energy and diffusion phenomena in the materials can lead to changes in macroscopic properties. However, particularly optical and mechanical applications require materials with a homogeneous distribution of the nanoparticles in the polymer matrix. In most of the cases a simple blending of fillers into high molecular weight (highly viscous) polymers is difficult, time-consuming and energy-intensive.[10] Hence, a chemical bottom-up route to class II materials is preferred due to a better control over the reaction parameters and consequently a higher homogeneity of the derived materials.

The sol–gel process is widely used in the preparation of class II hybrid materials due to its mild reaction conditions which leaves many possibilities for the compositional and structural design of mixed inorganic–organic materials.[11] A major process for the preparation of nanoscaled TiO_2 is sol–gel chemistry based on the hydrolysis and condensation of reactive titania precursors such as $TiCl_4$ or titanium alkoxides. Compared to the well-known silicon-based sol–gel process the controlled formation of metal oxides from transition metal alkoxides is much more difficult due to their higher precursor reactivity.[12,13] Coordination of bidentate ligands to metal alkoxides is regularly used to reduce the reactivity of the transition metal alkoxides by blocking coordination sites of the metal centers, while simultaneously introducing organic functionalities in the final material.[14] Thus, if the coordinating ligands are attached to a polymer chain, class II hybrid composite materials can be synthesized which consist of a metal oxide network and an organic polymer strongly interacted *via* a metal–ligand coordination.[15,16]

Polysiloxanes are a class of polymers interesting for many applications due to their unique properties, such as flexibility, low glass transition temperature (T_g), biocompatibility, high oxygen permeability, *etc.*[17,18] which makes them attractive for the synthesis of nanocomposite materials. Several studies reported the preparation of polysiloxane-metal oxide composite materials. Hybrid materials with good mechanical integrity and transparency consisting of hydrophobic and hydrophilic nanodomains have been prepared starting from

[a] *Vienna University of Technology, Institute of Materials Chemistry, Getreidemarkt 9, A1060 Vienna, Austria*
[b] *Vienna University of Technology, Institute of Materials Science and Technology, Favoritenstrasse 9-11, A1040 Vienna, Austria. E-mail: guido.kickelbick@tuwien.ac.at*

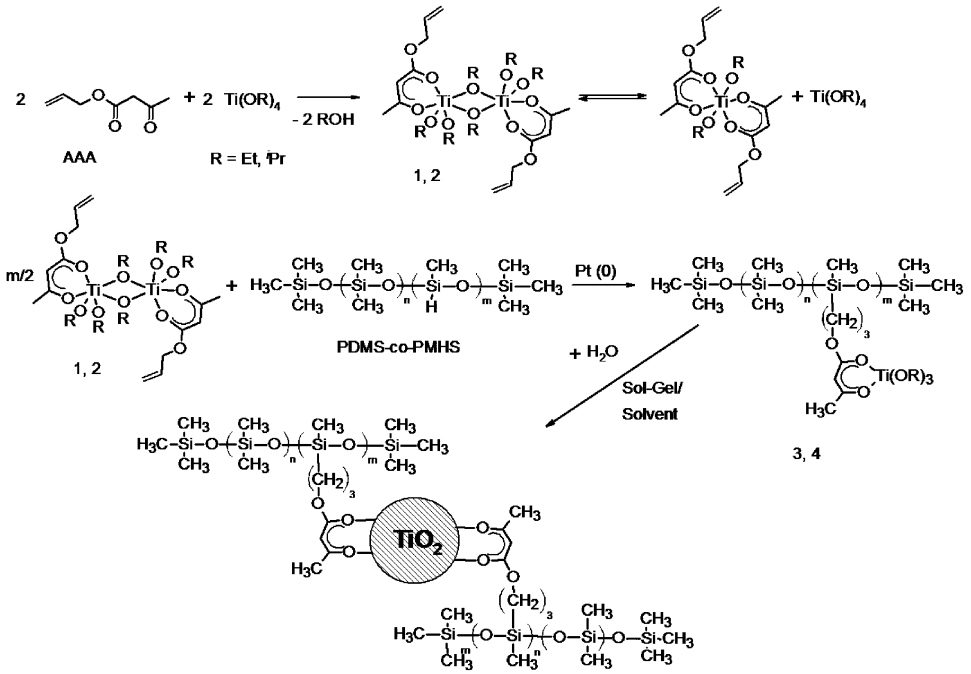

Scheme 1 The pathway for obtaining TiO_2-polysiloxanes hybrid materials (for clarity only monosubstituted AAA-$Ti(OR)_4$ modified polysiloxanes were drawn for the synthesis of the materials).

dimethyldiethoxysilane and zirconium alkoxides through sol–gel process.[19]

Hybrid materials based on the combination of TiO_2 and polydimethylsiloxanes (PDMS) have been also reported in the last years. Polydimethylsiloxane-TiO_2 materials prepared from titanium alkoxides and end-functionalized PDMS have been synthesized and reported to show interesting optical and elastic properties.[20–22] Hybrid TiO_2-PDMS particles with controlled refractive index were synthesized by a co-precipitation method starting from titanium isopropoxides and methoxy-functionalized PDMS.[22] In the same manner polydimethylsiloxane-metal-oxo nanocomposites constituted by metal-oxo nanodomains embedded in a PDMS matrix have been prepared as transparent monoliths from dimethyldiethoxysilane and different metal alkoxides (metal M = Al, Ge, Sn, Ti, Zr, Nb, and Ta). Depending on the nature of the crosslinking agent a different arrangement of the constituents of the hybrid composite was developed.[23,24]

It is well known that contrary to homopolymers like PDMS, block copolymers can show thermo- or lyotropic self-assembly[25,26] and the resulting aggregates have been successfully used as templates for the preparation of mesostructured materials.[27] Mesoporous silica structures and mesostructured silica and titania films can nowadays be synthesized using commercially available block copolymers as structure-directing agents.[28–30] Furthermore, the direct linkage of block copolymers to alkoxysilane groups can result in the formation of organic–inorganic nanohybrids when gelation occurs inside the alkoxysilane aggregates.[31] The idea of using the self-assembly of diblock copolymers led to the formation of highly ordered arrays of TiO_2 nanoparticles in a block copolymer matrix.[32] In such a way the design of new morphologically controlled architectures can be realized.

Here we report a novel route towards the synthesis of hybrid materials with a well-defined morphology. Our goal was to study the solvent induced aggregation phenomena of diblock polysiloxanes in order to design and control the morphology of titania-crosslinked polysiloxane hybrid materials.

Results and discussion

Formation of titanium alkoxide coordinated polysiloxanes

Titanium alkoxide functionalized polysiloxanes were prepared by coordinating the alkoxide *via* a β-keto ester to the block copolymer followed by the hydrolysis and condensation of the titanium alkoxide (Scheme 1). The first step was the coordination of the Ti alkoxide to allyl acetoacetate (AAA) by an exchange reaction of an alkoxide against the bidentate ligand and the following hydrosilation reaction of the formed coordination compound containing an unsaturated group with polydimethylsiloxane-*co*-polymethylhydrosiloxane (PDMS-*co*-PMHS). The reaction products of the ligand exchange reaction were investigated by means of NMR and FT-IR before hydrosilation. The coordination was proven by the disappearance of the typical β-keto ester signals (1745/1719 cm^{-1} (νC=O) and 1650/1636 cm^{-1} (νC=C)) and the presence of the chelating ligand absorption bands at 1633/1610 cm^{-1} (νC=C) and 1574/1524 cm^{-1} (νC=O) (Fig. 1). This coordination reaction takes place at room temperature by simply mixing the two compounds and stirring them. No bands of the free ligand were detected after 12 hours. In addition νTi-OR absorption bands were present between 620 and 500 cm^{-1} showing that the alkoxide moieties were still available for further reactions. ^{1}H NMR of Ti isopropoxides revealed the presence of the methine protons in the chelating ligand at 4.98 ppm. No signals of the uncoordinated ligand were detected supporting the full coordination of the allyl acetoacetate. ^{13}C

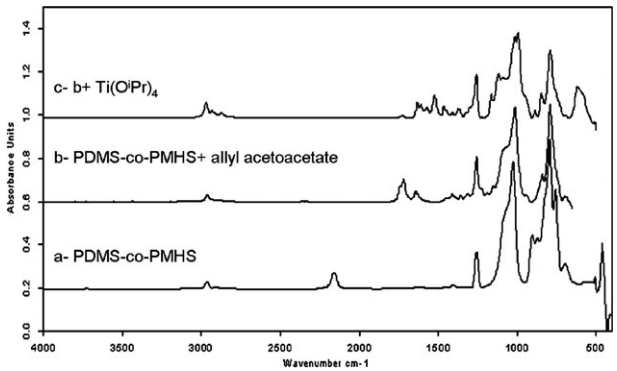

Fig. 1 The FT-IR analyses for the synthesis of the Ti alkoxides modified with polysiloxanes.

NMR shifts for the carbonyl atoms from the uncoordinated ligand (around 201 ppm/165.6 ppm) to the one of the chelating ligand (184 ppm/173.4 ppm) confirmed the ^{1}H NMR results.[33] Furthermore, no decomposition products which are possible side products formed by titanium alkoxide catalyzed transesterification reactions[34] were detected by the spectroscopic methods. In the solid state the formed compound is a binuclear centrosymmetric dimer consisting of two Ti atoms each coordinated by one chelating AAA and two terminal alkoxide ligands. In contrast, in solution an equilibrium between dimeric and monomeric, monosubstituted and disubstituted species is present resulting from redistribution reactions.[33,35]

Two different methods were used for the preparation of Ti alkoxide modified polysiloxane chains; either Ti alkoxides were coordinated to allyl acetoacetate in a first step and then hydrosilation with PDMS-*co*-PMHS was carried out, or attachment of allyl acetoacetate to the polymer *via* hydrosilation was applied in a first step followed by coordination of the Ti alkoxides to the thus modified polymer. The hydrosilation reaction of $[Ti(OR)_3AAA]_2$ with poly(dimethylsiloxane)-*co*-(methylhydrosiloxane) (PDMS-*co*-PMHS) was carried out over night resulting in complete conversion of the Si-H groups using Pt(0) Karstedt catalyst. The reaction progress was monitored by FT-IR and NMR. It was obvious from the IR spectra (Fig. 1) that the coordination of the β-keto ester to the titanium atoms is maintained after the hydrosilation by the presence of the specific bands of the chelating ligand (νC=C: 1633/1610 cm^{-1}, νC=O: 1574/1524 cm^{-1}) in the final product. Additionally, the completeness of hydrosilation was proven by the disappearance of the Si-H band at around 2160 cm^{-1} in the IR as well as its corresponding peak in the ^{1}H NMR at 4.72 ppm and the olefin protons of the allyl acetoacetate ligand (5.86/5.19 ppm). 2D NMR (HSQC, HMBC, and COSY) spectroscopy confirmed these results. The full disappearance of the signals corresponding to the allyl moieties was complemented by the appearance of two new methylene signals in the ^{13}C NMR corresponding to the formed –Si–CH_2–CH_2–CH_2O linker (13.3, 22.6 ppm).

The second pathway, *i.e.* attachment of the ligand and afterwards coordination of the metal alkoxide, gave similar results with regard to the hydrosilation reaction. Coordination of the modified polysiloxane with Ti alkoxides was as well accomplished under the same conditions as for the analogue coordination with the allyl acetoacetate. The first method was chosen as the standard procedure. The second procedure has the disadvantage that the control over the coordination of the metal alkoxides was not easy to obtain because of the crosslinking that occurred immediately after mixing the polymer and the metal alkoxides. It is difficult to control the crosslinking reaction which makes the reproducibility of the results problematic. Therefore we focused on the first pathway.

Synthesis of the nanoparticles

The sol–gel process is usually carried out in the alcohols corresponding to the alkoxide ligands of the metal alkoxides. However, polysiloxanes are known to show a low solubility particularly in short chain alcohols.[36] For example, the swelling of PDMS if infiltrated with ethanol is rather low, compared to a lower polarity solvent such as toluene.[37] Hence, ethanol as a non solvent for PDMS usually leads to a minimization of the interface between the solvent and the polymer chain and thus the formation of a coil-like arrangement on a molecular scale as well as phase separation on the macroscale. The idea behind our synthetic strategy was to fix this coil-like arrangement through a crosslinking reaction induced by the sol–gel process of the coordinated titanium alkoxides.

Hybrid nanoparticles were obtained applying a sol–gel process to the titanium alkoxide-modified polysiloxane precursors in the corresponding alcohol as solvent overnight. The ratio between Ti atoms and water was varied from 1:1 to 1:3 in order to determine if higher water content would lead to a higher condensation ratio of the alkoxides, hence to larger particles. Hoebbel *et al.* investigated the hydrolysis behavior of the complex between allyl acetoacetate ligands and different metal alkoxides (Ti, Zr, Al alkoxides) under sol–gel conditions. They observed a dissociation of 15% of the AAA ligand from the complex for a ratio between H_2O and alkoxide ligands in the empirical formula $Ti(OR)_3AAA$ of 1 ($Ti:H_2O$ = 1:3).[38] Our investigations focused on smaller ratios between Ti and H_2O equal to 1.5 to guarantee the maintenance of the chemical bond between the polysiloxane chains and the titanium atoms during hydrolysis and condensation. The addition of pure titanium alkoxide in a 1:1 ratio to the modified polysiloxanes and its influence on the composition and morphology of the final materials was investigated as well. The particles were centrifuged and dried under vacuum and their chemical structure was explored by NMR and FT-IR spectroscopy. FT-IR analyses revealed that the characteristic bands of the chelating ligand between 1640 and 1525 cm^{-1} are maintained after hydrolysis which proves the existence of a linkage between the Ti atoms and the polysiloxanes. The specific absorption bands of the polysiloxanes were detected at 1024 cm^{-1} and 791 cm^{-1}. The ^{13}C CP/MAS NMR and ^{29}Si CP/MAS NMR spectra of the same sample are presented in Fig. 2 and 3.

The ^{13}C CP/MAS NMR spectrum revealed the presence of the typical carbonyl signals of the chelating form of the allyl acetoacetate ligand at 177.2 ppm and 165.7 ppm and the presence of the methine (CH) carbons of the chelating ligand at 81.8 ppm. These values correspond well to the ones of the

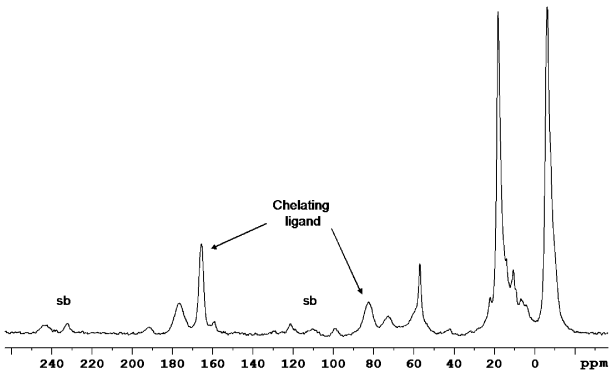

Fig. 2 The ^{13}C CP MAS NMR spectrum of the TiO_2-polysiloxane nanoparticles (sb-sidebands).

chelating ligand in the soluble complex measured in liquid state proving that coordination is maintained after the sol–gel process. The presence of the polysiloxanes in the final nanoparticles is supported by the signal at −6.4 ppm corresponding to the methyl carbon atoms of the main polymer chain. The connection between the polysiloxane chain and the chelating part of the ligand is proven by the presence of the methylene atoms at 14.1 ppm. The ^{29}Si CP/MAS NMR spectra revealed the presence of the end groups in the **M** region (6.7 ppm). The Si atoms from the main chain resulted in a signal in the **D** region (–22.51 ppm). The signals between −62 and −68 ppm may be due to some **T** type Si atoms which are resulting as a side-reaction of the hydrosilation process (O-silylation due to moisture).[39,40]

Dynamic light scattering (DLS) analyses showed that most of the samples present an unweighted bimodal distribution function with sizes between 3–15 nm (1st mode) and 45–100 nm (2nd mode) (Fig. 4). The larger size distributions can be explained by agglomeration or by the different molecular aggregates due to the fact that the Ti compounds with β-keto esters present a dynamic equilibrium in solution between different species.[33] However, after weighting of the peaks (number and mass weight) it was obvious that the majority was represented by the small size particles and the larger agglomerates sum up to <25% of the total amount of colloids in the suspension. In the cases of polysiloxanes modified with Ti isopropoxides we observed that the ratio between the two distributions were dependent on the

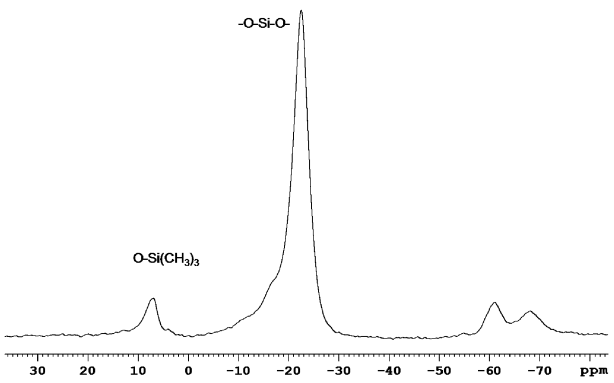

Fig. 3 The ^{29}Si CP MAS NMR spectrum of the TiO_2-polysiloxane hybrid nanoparticles.

concentration of the precursor (modified polysiloxanes). The quantifications were made by the mass weighting of the distribution functions obtained by DLS. Different measurements were carried out in a concentration range between 0.01 and 0.0275 mol/L precursor. The percentage of particles with a radius of 2.72 ± 0.1 nm (the 1st distribution function) was approximately 100% for a concentration of 0.018 mol/L modified polysiloxane in ethanol while for a precursor concentration of 0.02 mol/L the percentage of particles with 4 ± 0.2 nm radius (1st distribution function) was 89% (Fig. 4). No nanoparticles were obtained for high concentrations of modified polysiloxanes (>0.04 mol/L). The increase of the particle size with the increase of the alkoxide concentration is due to the fact that the probability of particles that merge and form a novel particle is higher than in the cases of more diluted solutions, so agglomeration occurs in very early stages of the sol–gel process.

With the increase of the water content the nanoparticle size distribution function broadens significantly which makes the determination of the particle radii by DLS not possible. This observation is most likely due to the hydrolysis of the β-keto ester moieties which increase the reactivity of the titanium alkoxides, thus leading to a more uncontrolled growing process. The addition of $Ti(O^iPr)_4$ in a 1:1 ratio with regard to the Ti content to Ti-modified polysiloxanes resulted in different particle distributions at 139 nm and 1.618 μm radius. Both of the distribution functions were broad. In this case, the increase in the particle size is due to the high reactivity of the Ti alkoxides in the sol–gel reaction. A comparison between different titanium alkoxides showed that smaller particle radii were obtained for $Ti(O^iPr)_4$ than for $Ti(OEt)_4$. This can be due to either a steric effect of the bulky isopropoxy groups hindering the growth of the particles, or the different equilibrium between monomeric and dimeric species in this case.[33]

We expected the formation of the nanoparticles to be strongly influenced by the interactions of the PDMS chains with the solvent. The PDMS chains have a low solubility in ethanol[36] causing the PDMS-PHMS copolymers to form coils minimizing the interface to the incompatible environment. DLS measurements of the polysiloxanes in ethanol revealed that the size of these coils is around 2 nm in diameter (Fig. 5). After modification with the titanium alkoxides and carrying out the sol–gel process this architecture is frozen by the condensation of the Ti alkoxides. The growth of the nucleation centers is hindered by the PDMS chains.

Ti alkoxide-modified polysiloxanes in ethanol have diameters that are only insignificantly larger than the unmodified systems. After sol–gel process the diameter of the particles is doubled (~6 nm ± 1). The dispersions are stable and no agglomeration or precipitation was observed. DLS is not able to provide information on the morphology of the particles, because the theory assumes a spherical nature of the particles. As mentioned above the nanoparticles were stable after purification for several weeks when dispersed in ethanol but they precipitate after a few days when left in the reaction mixture. This can be due to the further condensation of the not reacted alkoxides as well as to the hydrolysis of the ligands, leading to agglomeration and precipitation. Transmission electron microscopy (TEM) analyses confirm the formation of nanoparticles. Fig. 6 presents a characteristic TEM image of the

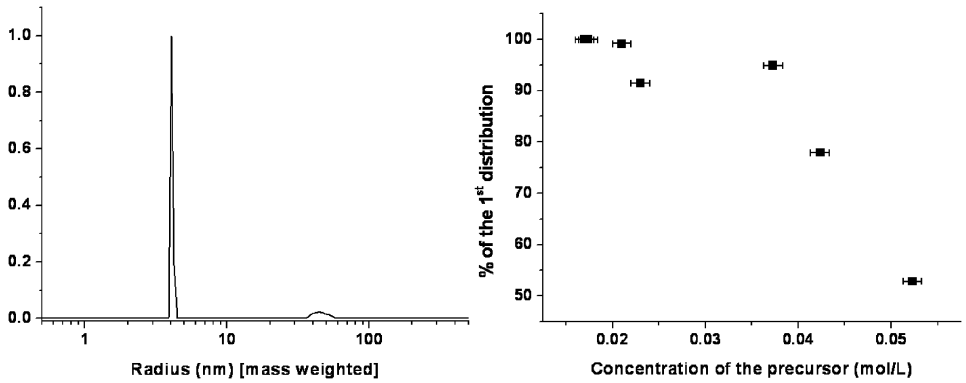

Fig. 4 The DLS distribution function mass weighted (left) and the concentration dependence of the ratio between the two particle sizes.

hybrid nanoparticles and the size distribution calculated from the same image by counting and measuring 50 particles.

TEM showed the presence of particles and agglomerates with diameters ranging from 10 to 80 nm with a main distribution at around 45 nm. This confirms the DLS measurements if we also consider the fact that the bigger sizes were probably due to agglomeration after the evaporation of the solvent upon the deposition of the particles on the copper grid.

Scanning electron microscopy (SEM) also showed the presence of agglomerates of small particles with diameters around 30 nm. Energy dispersive X-ray (EDX) analysis showed that these nanoparticles contained both Ti and Si atoms. This fact proved the hybrid nature of the nanoparticles (Fig. 7).

Atomic force microscopy (AFM) was used to further characterize particles after deposition on a clean mica surface. Use of the dynamic (or tapping) mode allowed the acquisition of phase images which nicely complements the high resolution topographical information obtained by classical contact mode. Fig. 8 presents a representative AFM image containing both the topographic and the phase information. The clear phase contrast between the particle center and the edge further supports the hybrid core-shell morphology. The topographic analysis shows that the core of the larger particles clearly consists of agglomerates of many small-sized particles. The line scans through the core and the shell of the particles show that while the polysiloxane shell forms a thin layer with a thickness of roughly 2 nm on the mica surface, the core consisting of agglomerated particles has a relatively irregular morphology with sample height ranging from 10 up to 18 nm. The large height difference results from the fact that the particles are deposited and dried on a surface. This leads to a collapse of the polysiloxane shell which is expected to extend homogeneously and spherically around the TiO_2 core when dispersed in a solvent.

The largely oxidic core, on the other hand, remains virtually unaffected by the drying process. As seen in Fig. 9, in addition to the large particles many smaller particles were encountered on the same sample substrate surface showing very similar core-shell morphology. Throughout the prepared samples this shell exhibits a phase contrast to the particle core representing the chemical difference between the TiO_2 core and the polysiloxane shell.

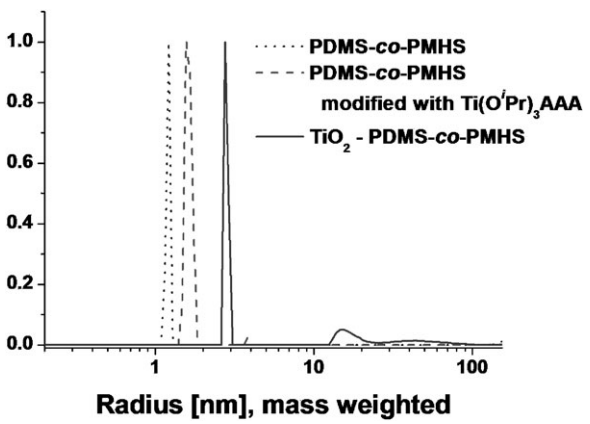

Fig. 5 DLS distribution function of PDMS-co-PMHS (dot), PDMS-co-PMHS modified with $[Ti(O^iPr)_3AAA]_2$ (dashed) and TiO_2-polysiloxanes hybrid nanoparticles (line) in ethanol.

Synthesis of the gels

Our hypothesis that the solubility of the PDMS chains in ethanol is the main driving force in the formation of the hybrid nanoparticles was sustained by the synthesis of TiO_2-polysiloxane gels switching the solvent to toluene, where polysiloxanes show a high solubility. Applying the sol–gel process to the polysiloxanes modified with the Ti alkoxides under the same conditions as above mentioned, solid opaque gels were obtained. The gels were analyzed by means of NMR and FT-IR spectroscopy. The coordination between the titanium and the acetoacetate ligand is still maintained, being confirmed by the presence of the chelating bands of the ligand at 161a cm^{-1} ($\nu C{=}C$) and 1528 cm^{-1} in the IR spectrum. Also the incorporation of the polysiloxanes in the final gel is sustained by the presence of the specific absorption bands of the polysiloxanes at 1024 cm^{-1} and 792 cm^{-1}. ^{29}Si CP/MAS NMR spectrum revealed the presence of the end groups in the M region (6.7 ppm) and the Si atoms from the main chain gave a signal in the **D** region (−22.8 ppm). All characteristic signals of the chelating ligand were present in the ^{13}C CP/MAS NMR spectra and no traces of residual alkoxides were identified. The wet gels were stable for months when kept in toluene or ethanol. Even if in the first hours of the sol–gel reaction the presence of nanoparticles was observed by DLS, the TEM analysis showed that the gels were uniform and no presence of separate domains was observed, proving that the polysiloxanes were uniformly included in the titanium oxide matrix.

Xerogels were prepared from the TiO_2-polysiloxane hybrid gels by drying at room temperature for several days. The obtained xerogels were amorphous as observed by X-ray

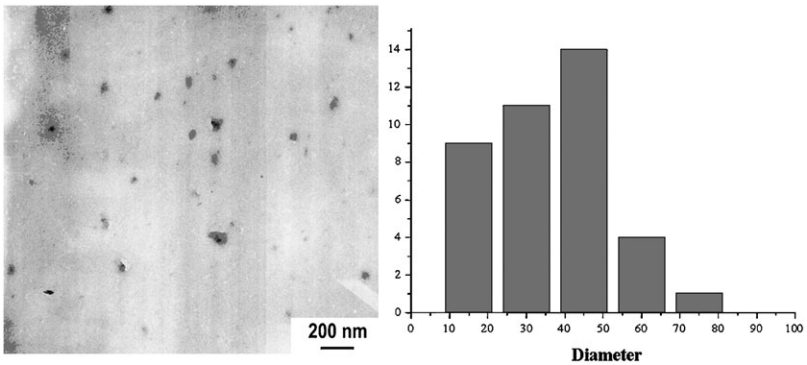

Fig. 6 TEM image of the TiO_2-polysiloxanes hybrid nanoparticles and the size distribution calculated from the picture.

diffractometry. After calcination at 800 °C for several hours X-ray powder diffraction measurements showed the presence of both anatase and rutile TiO_2 phases.

AFM analysis of the TiO_2-polysiloxane gels revealed only very large particles which showed no evidence of a core-shell morphology. This is in accordance with the fact that in this case the particle growth is not restricted, thus leading to the formation of homogenous gels containing polysiloxane titania interpenetrating networks.

SEM analysis of the xerogels dried at room temperature before calcination showed no presence of ordered pore structures. Instead the images revealed spherical domains present on the surface of the hybrid xerogels (Fig. 11). The surface between the domains showed an interesting rippled texture. EDX was conducted on the same sample in order to establish the composition of the xerogels and also to see if the observed dimples are metal oxide agglomerates or just due to the evaporation of the solvent. The interesting fact to find out was if the surface domains (which were perfectly symmetric to each other and showed the same diameters, with a star-like shape) are a defect of the surface or if they are formed regularly during the sol–gel process. Because the samples were sputtered with a thin gold layer for better conductivity the EDX results could not be quantified. Also the analysis of light elements (carbon, oxygen) is problematic in EDX. However the results were well reproducible so that some general statements could be given. The analyses revealed that the main matrix (a) is basically composed from Si, Ti, O and C. In the case of the 'star-shape domains' the ratio between Si and Ti was similar to the one from the matrix. The only difference was a higher content of carbon in the round 'domain' compared to the surrounding matrix. This is most likely due to the evaporation of the solvent during the slow drying at room temperature. However these results show that a hybrid xerogel is formed, containing both the metal oxide and the polymer highly dispersed into each other.

A mechanism for the structure formation of the samples can be formulated from the results obtained for the different prepared samples (Scheme 2). As shown by the DLS investigations of the unmodified block copolymers, the PDMS chains are not well soluble in alcohol forming coil like moieties in this solvent. This architecture can be fixed by the sol–gel reaction of the Ti alkoxide-modified polysiloxanes as proven by DLS, TEM and AFM. Toluene is a good solvent for the PDMS chains. They are much more expanded in this solvent and the sol–gel process leads to crosslinked networks.

Conclusions

A pathway for the modification of different polysiloxanes with metal alkoxides was presented. The coordination between allyl acetoacetate and different Ti alkoxides afforded well-defined compounds which were linked to a polymer chain *via* the hydrosilation reaction of the Si–H bonds with the allyl moieties. The investigation showed that the coordination between the β-keto esters and the Ti alkoxides was not disturbed by the hydrosilation. The structure of these copolymers was investigated by FT-IR and NMR which showed the complete functionalization of the polysiloxane chains with the metal

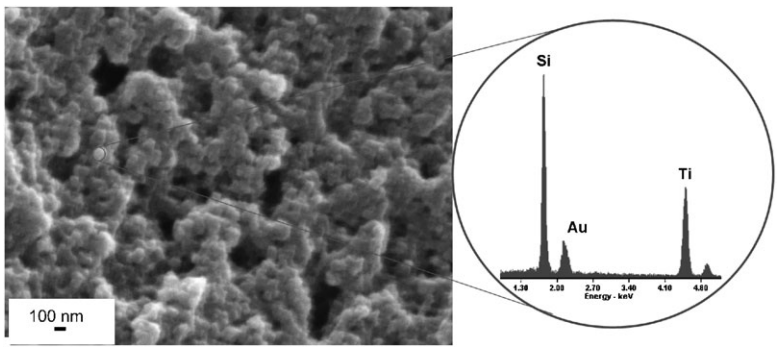

Fig. 7 SEM image and EDX analyses of the TiO_2-polysiloxane hybrid nanoparticles.

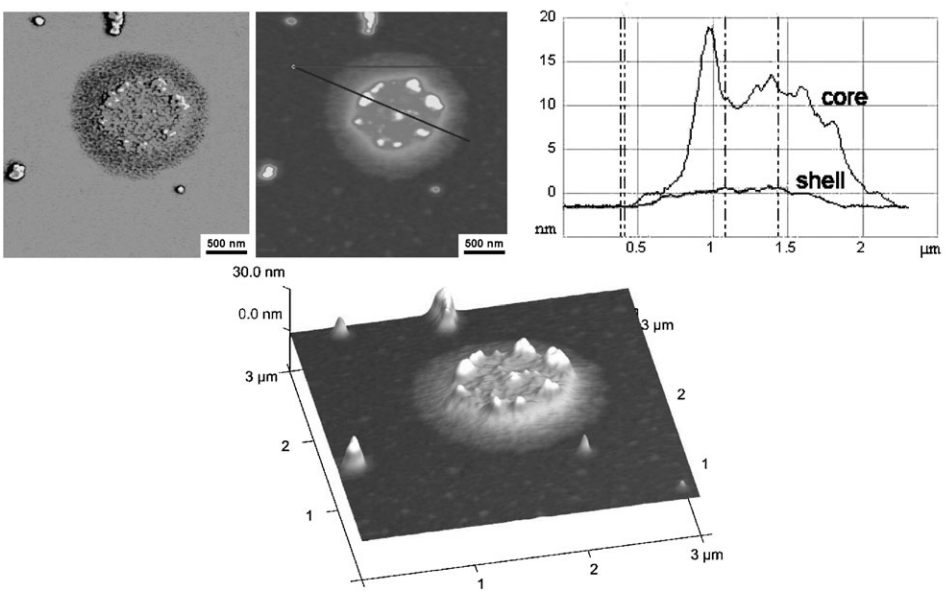

Fig. 8 AFM images of TiO_2-polysiloxane nanocomposite particles; top: phase image (left); topographic image (center) with the lines indicating the sections through the image (right); bottom: 3D topographic representation of the particle.

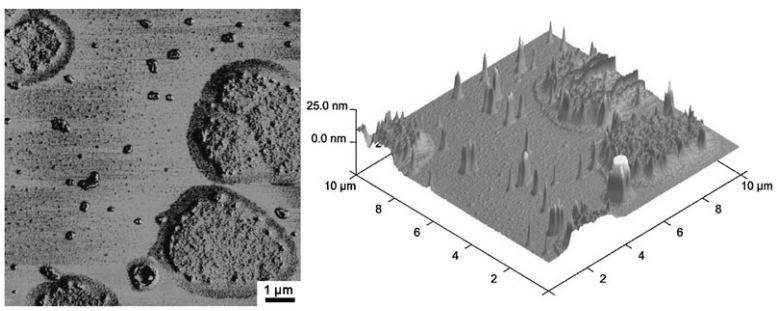

Fig. 9 AFM phase image (left), and the corresponding 3D topographic image of the TiO_2-polysiloxane nanoparticles.

alkoxides. Hybrid nanoparticles or gels were obtained by applying sol–gel conditions to the modified polymers. Nanoparticles were obtained when alcohols were employed as solvents. This was due to the fact that PDMS chains have a poor solubility in polar solvents and they tend to form micelle type aggregates as shown by DLS. The investigation of the structure of the nanoparticles by FT-IR and solid-state NMR showed that the linkage between the polymer chains and the metal oxide was maintained *via* the coordinative β-keto esters. The DLS measurements showed that the particles had a radius between 3 and 15 nm. Most of the samples presented a bimodal size distribution, with a second distribution function between 70 and 100 nm radii. The percentage of the second, larger-sized distribution mode was very low at small precursor concentrations and increased with increasing concentration. The TEM, SEM, and AFM analyses sustained the formation of the hybrid nanoparticles. By contrast, hybrid gels were obtained when toluene was employed as a solvent in the sol–gel process. This was due to the fact that the PDMS chains were well soluble and the nucleation centers could grow to form a homogeneous, continuous phase. The chemical analyses showed that the polysiloxane was incorporated in the oxide matrix. The SEM analyses of the xerogels show uniform surfaces with no presence of pores.

Fig. 10 TiO_2-polysiloxane hybrid gel photograph.

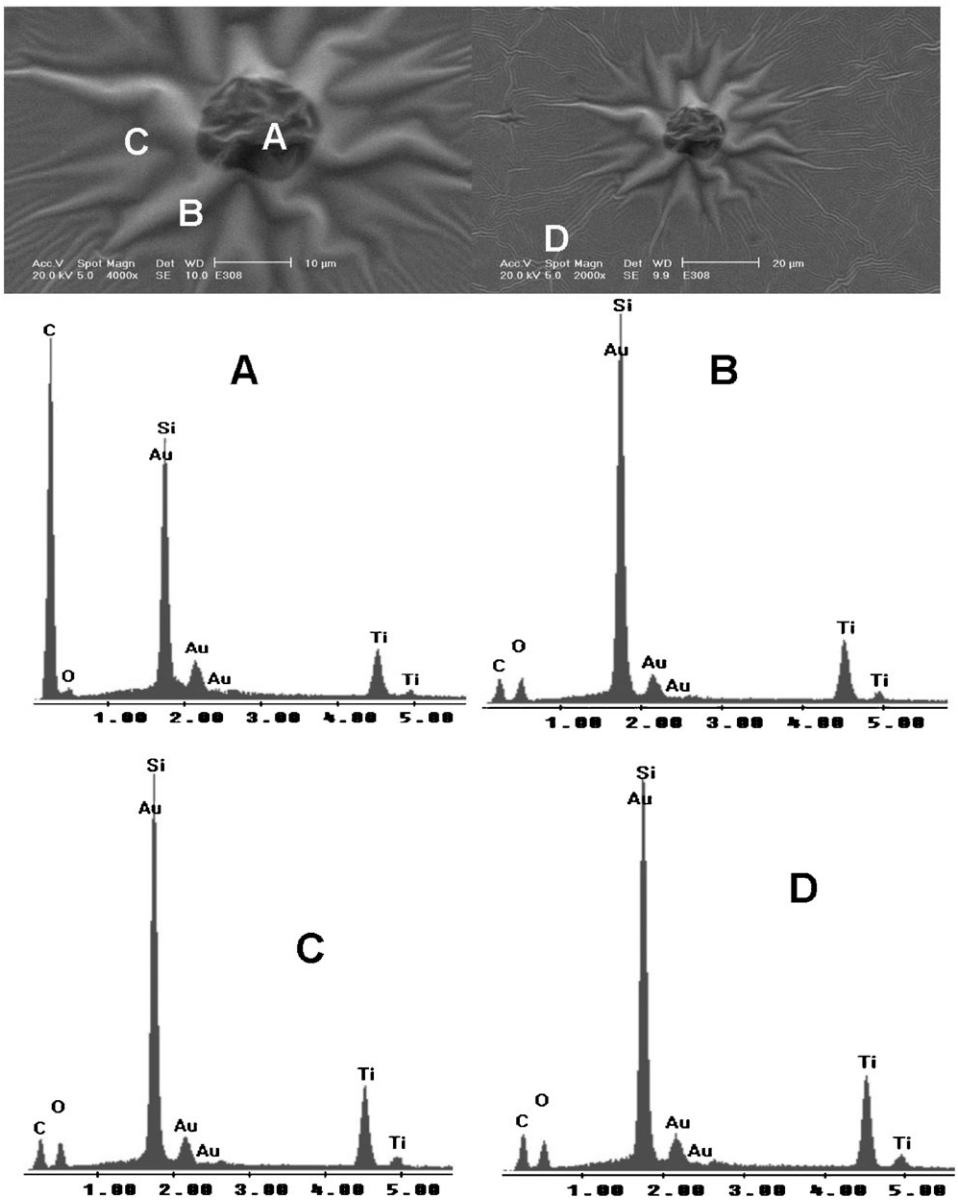

Fig. 11 SEM images and EDX analyses of the TiO_2-polysiloxane hybrid xerogels.

Experimental

Measurements

Solution NMR spectra were recorded on a Bruker Avance 300 (^{1}H at 300.13 MHz, ^{13}C at 75.47 MHz) equipped with a 5 mm inverse-broadband probe head with a *z*-gradient unit. 2D-experiments were measured with Bruker standard pulse sequences (COSY (Correlated Spectroscopy), TOCSY (Total Correlation Spectroscopy), HSQC (Heteronuclear Single Quantum Correlation), HSQC-TOCSY, HMBC (Heteronuclear Multi Bond Correlation)). Solid State NMR spectra were recorded on a Bruker DPX 300 (^{13}C at 75.40 MHz) equipped with a 4 mm broadband MAS probe head. ^{13}C and ^{29}Si NMR spectra were recorded with ramped CP/MAS spectra (Cross Polarization and Magic angle spinning). Rotor spinning speed was usually 6–8 kHz. FT-IR spectra were recorded on a Bruker Tensor 27 instrument working in ATR MicroFocusing MVP-QL with a ZnSe crystal. The software used for analysis was OPUS™ version 4.0. The dynamic light scattering measurements were performed with an ALV/CGS-3 compact goniometer system with an ALV/LSE-5003 light scattering electronics and multiple τ digital correlator at 25 °C. Samples for transmission electron microscopy (TEM) measurements were prepared by ultrasonically dispersing the particles in ethanol prior to deposition on a carbon coated TEM Cu-grid. TEM measurements were performed on a JEOL JEM-200CX or a JEOL JEM-100CX at the University Service Centre for Transmission Electron Microscopy, Vienna University of Technology, Austria. Samples for atomic force microscopy (AFM) were prepared by ultrasonically dispersing the particles in ethanol prior to deposition on a freshly cleaved mica surface. AFM images were recorded using a NanoScope III Multimode SPM by Veeco Instruments. Measurements were performed in air in tapping, constant amplitude mode using silicon cantilevers with integrated silicon tips (NanoWorld, spring constant 42 N/m, resonance

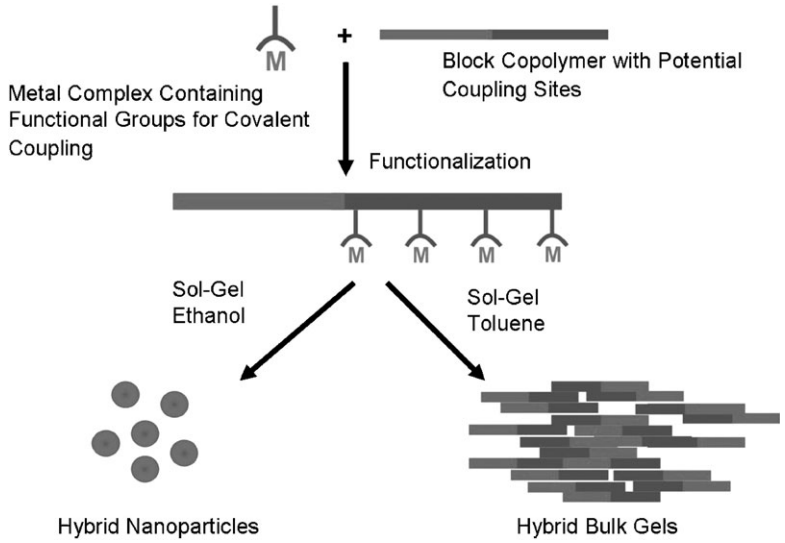

Scheme 2 The possible mechanism in the synthesis of TiO_2 modified with polysiloxane nanoparticles and gels.

frequency ~285 kHz). All images were recorded with a resolution of 512 × 512 pixels at scanning rates of 0.5–5.0 Hz, depending on the size of the selected scan area. Data analysis was performed using the commercial NanoScope software. Scanning electron microscopy (SEM) imagines were recorded on a Philips XL-30. The samples were sputtered on the surface with a thin gold layer prior to SEM imaging. For measurements secondary electrons were used. The typical conditions (accelerating voltage, magnification *etc.*) can be seen on the pictures.

Materials

Titanium tetraisopropoxide ($Ti(O^iPr)_4$, 97%, Aldrich), titanium tetraethoxide ($Ti(OEt)_4$, purum, Fluka), allyl acetoacetate (AAA, 98%, Aldrich), poly(dimethylsiloxane-*co*-methylhydrosiloxane) 50:50 (PDMS-co-PMHS, average M_n ~ 950, methylhydrosiloxane 50 mol%, Aldrich), polyhydromethylsiloxane (PMHS, 97%, average M_n = 1700–3200, Aldrich), Pt(0) (Platinum(0)-1,3-divinyl-1,1,3,3-tetramethyldisiloxane complex solution, 0.1 M in poly(dimethylsiloxane), vinyl terminated, Aldrich) catalyst were used as received. Toluene was dried over sodium metal and distilled freshly before usage. Ethanol was dried using magnesium and distilled afterwards.

Coordination of Ti alkoxides with AAA. The synthesis was based upon a literature known procedure.[33] AAA (1.58 mL, 11.5 mmol) was added to a solution of $Ti(OEt)_4$ (2.62 g , 11.5 mmol) or $Ti(O^iPr)_4$ (3.26 g, 11.5 mmol) in 20 mL of hexane. The reaction was stirred over night. Removal of the solvent in vacuum gave **1** and **2** as yellow solids (2.7 g, 75%).

$[Ti(OEt)_3CH_3C(O)CHC(O)OCH_2CH{=}CH_2]_2$ (1). ^{1}H NMR (25 °C, $CDCl_3$, ppm). CH_3CH_2O–: 1.22(t), J = 6.75 Hz, CH_3CO: 1.98(s), 1.91(s), OCH_2CH_3: 4.47(m), 4.79(m,br) CH_2CO: 4.63–4.74(m,br), $COCHCO$: 5.02(s), $=CH_2$: 5.17–5.33(m), $-CH=$: 5.78–5.99(m). ^{13}C NMR ($CDCl_3$, 25 °C, ppm): CH_3CH_2O–: 18.2; CH_3CO: 25.0; OCH_2CH_3: 71.3; CH_2O: 72.8; $(CO)_2CH$: 88.6; $=CH_2$: 117.5; $CH=$: 133.8; CH_3CO: 174.8; COO: 185.3. Selected FT-IR bands (ATR, cm^{-1}): (νC=C): 1634/1611, (νC=O): 1574/1524.

$[Ti(O^iPr)_3CH_3C(O)CHC(O)OCH_2CH{=}CH_2]$ (2). ^{1}H NMR (25 °C, $CDCl_3$, ppm). $(CH_3)_2CHO$: 1.24(d), J = 6.1 Hz, CH_3CO: 1.94(s), 1.85(s), $(CH_3)_2CH$: 4.46 (sept), J = 5.7, 11.87 Hz, CH_2O: 4.76(d), J = 6.06 Hz, $COCHCO$: 4.98(s), $=CH_2$: 5.26(m), $-CH=$: 5.76–5.92(m). ^{13}C NMR ($CDCl_3$, 25 °C, ppm): $(CH_3)_2CHO$: 22.0; CH_3CO: 25.12; $=CHCH_2O$: 73.2; $(CH_3)_2CH$: 79.2; $(CO)_2CH$: 88.7; $=CH_2$: 117.8; $CH=$: 133.4; CH_3CO: 174.0; COO: 184.7. Selected FT-IR bands (ATR, cm^{-1}): (νC=C): 1636/1612, (νC=O): 1576/1529.

Hydrosilation of poly(dimethylsiloxane)-co-poly(methylhydrosiloxane) (50:50) with AAA and coordination with $Ti(O^iPr)_4$ or $Ti(OEt)_4$. A solution of Si–H functionalized polysiloxanes and allyl acetoacetate (1 mol/mol Si–H groups) in absolute toluene was stirred at room temperature under argon atmosphere. The coupling reaction was carried out by applying 10^{-4} mol Pt(0) catalyst (Karstedt catalyst). The reaction was further stirred over night. After the analysis of the product $Ti(O^iPr)_4$ was added (1:1 ratio with respect to the ligand) and the solution was stirred further overnight. The results for the formation of the polymers are given in the next paragraph.

Hydrosilation of $[Ti(OEt)_3AAA]_2$ and $[Ti(O^iPr)_3AAA]_2$ with poly(dimethylsiloxane)-co-(methylhydrosiloxane) (50:50) (3, 4). To a solution of $[Ti(OR)_3AAA]_2$ (7.98 g, 10.9 mmol) and polysiloxane containing Si–H bonds (2 mL, 2.08 mmol) in toluene a few drops of Karstedt catalyst were added (10^{-4} mol). The reaction was stirred overnight and the solvent was removed in vacuum. The reaction was monitored by the disappearance of the Si–H signal in FT-IR and NMR (described in Results and Discussions).

$[Ti(OEt)_3AAA]$-PDMS-co-PMHS (3). ^{1}H NMR ($CDCl_3$, 25 °C, ppm). CH_3Si: 0.08(s, br), $SiCH_2$: 0.51(m), CH_3CH_2O–: 1.20–1.23(m, br), $SiCH_2CH_2$: 1.60–1.88(m, br), CH_3CO1.91(s), CH_2CO: 3.71–3.82 (m, br), CH_3CH_2O–: 4.47(m), $COCHCO$: 4.98(s). ^{13}C-NMR ($CDCl_3$, 25 °C, ppm): CH_3SiO: –0.689; CH_2CH_2Si: 11.7; CH_3CH_2O– 18.2; $SiCH_2CH_2$: 22.4; CH_3CO: 25.0; $SiCH_2CH_2CH_2$: 66.9; CH_3CH_2O: 73.1; $(CO)_2CH$: 88.7/90.8; CH_3CO: 174.2; COO: 185.1. ^{29}Si NMR,

($CDCl_3$, 25 °C, ppm): $(CH_3)_3SiO$: 6.12, OSiO: –22.78. Selected FT-IR bands (ATR, cm^{-1}): (C═C): 1638/1610, (C–O): 1570/1524, (CH): 1258, (Si–O–Si): 1023, (C–Si–C): 788.

[Ti(O^{i}Pr)$_3$AAA]-PDMS-co-PMHS (4):. ^{1}H NMR($CDCl_3$, 25 °C, ppm). CH_3Si: 0.09(s, br), SiCH_2: 0.56(m), $(CH_3)_2$-CHO– 1.19–1.26(m, br), $SiCH_2CH_2$: 1.51–1.68(m, br), CH_3CO: 1.93(s), CH_2CO: 4.02–4.27(m, br), $(CH_3)_2CH$: 4.49 (sept), J = 6.01, 11.78 Hz, 4.75(sept), J = 5.21, 11.45 Hz, COCHCO: 4.95(s). ^{13}C-NMR ($CDCl_3$, 25 °C, ppm): CH_3SiO: −2.18; CH_2CH_2Si: 13.3; $(CH_3)_2$CHO–: 22.0; $SiCH_2CH_2$: 22.6; CH_3CO: 25.12; $SiCH_2CH_2CH_2$: 64.76; $(CH_3)_2CH$: 79.2; $(CO)_2CH$: 86.8/88.6; CH_3CO: 174.1; COO: 184.4. ^{29}Si NMR, ($CDCl_3$, 25 °C, ppm): $(CH_3)_3SiO$: 6.4, OSiO: −22.85. Selected FT-IR bands (ATR, cm^{-1}): (C═C): 1633/1610, (C–O): 1574/1524, (CH): 1259, (Si–O–Si): 1023, (C–Si–C): 788.

Sol–gel reaction in ethanol: synthesis of hybrid nanoparticles. The Ti-modified polysiloxanes (typically between 0.1 and 0.6 mmol modified polymer) were dissolved in ethanol (THF was also successfully used) and water was added under vigorous stirring in different ratios (from 1:1.5 to 1:3) with regard to the Ti content. The solution was stirred overnight (12 hours). The products were centrifuged, washed three times with methanol and water and redispersed in ethanol or dried and analyzed by NMR and FT-IR. ^{13}C CP/MAS (25 °C, ppm): CH_3SiO: −6.4; CH_2CH_2Si: 14.1; $SiCH_2CH_2$: 18.3; CH_3CO: 22.2; $SiCH_2CH_2CH_2$: 57.1; $(CO)_2CH$: 81.8; CH_3CO: 165.7; COO: 177.2. ^{29}Si CP/MAS (25 °C, ppm): $(CH_3)SiO$: 6.7, $OSi(Me)_2O$: −22.5. FT-IR (25 °C, ATR, cm^{-1}): (C═C): 1610, (C–O): 1528, (CH): 1260, (Si–O–Si): 1025, (C–Si–C): 792.

Sol–gel reaction in toluene: synthesis of hybrid gels. TiO_2 modified polysiloxane gels were obtained when the sol–gel reaction of the alkoxide modified polysiloxanes was carried out in toluene as solvent using the same water ratio as for the synthesis of the nanoparticles. The sol–gel reactions were carried out over night and the mixtures were placed in cylindrical glass vials for gelation. Gels were obtained at room temperature after two days.

Synthesis of TiO_2-polysiloxane xerogels. The TiO_2-polysiloxanes hybrid gels were dried at room temperature for several days. ^{13}C CP/MAS (25 °C, ppm): CH_3SiO: −0.4; CH_2CH_2Si: 16.0; $SiCH_2CH_2$: 23.7; CH_3CO: 26.7; $SiCH_2CH_2CH_2$: 61.5; $(CO)_2CH$: 85.7; CH_3CO: 171.4; COO: 181.7. ^{29}Si CP/MAS: $(CH_3)SiO$: 6.73, $OSi(Me)_2O$: −22.75. FT-IR (25 °C, ATR, cm^{-1}): (C═C): 1635/1611, (C–O): 1576/1529, (CH): 1260, (Si–O–Si): 1025, (C–Si–C): 792.

Acknowledgements

Financial support of this work by the Austrian Fonds zur Förderung der wissenschaftlichen Forschung (FWF, Project nr.: P17424) is gratefully acknowledged. We thank Dr Johannes Bernardi and the USTEM at the Vienna University of Technology for assistance during electron microscopy studies and Prof. Gernot Friedbacher from the Institute of Chemical Technologies and Analytics at the Vienna University of Technology for assistance during AFM studies.

References

1. C. Sanchez, B. Julian, P. Belleville and M. Popall, *J. Mater. Chem.*, 2005, **15**, 3559–92.
2. G. Kickelbick, *Hybrid Materials. Synthesis, Characterization, and Applications*, Wiley-VCH Verlag GmbH & Co., New York, 2007.
3. G. Kickelbick, *Prog. Polym. Sci.*, 2002, **28**, 83–114.
4. J. Boucle, P. Ravirajan and J. Nelson, *J. Mater. Chem.*, 2007, **17**, 3141–53.
5. J. Pena, M. Vallet-Regi and J. San Roman, *J. Biomed. Mater. Res.*, 1997, **35**, 129–34.
6. X. Chen and S. S. Mao, *J. Nanosci. Nanotechnol.*, 2006, **6**, 906–25.
7. A. G. Agrios and P. Pichat, *J. Appl. Electrochem.*, 2005, **35**, 655–63.
8. B. L. Cushing, V. L. Kolesnichenko and C. J. O'Connor, *Chem. Rev.*, 2004, **104**, 3893–946.
9. T. Furuzono, M. Iwasaki, S. Yasuda, A. Korematsu, T. Yoshioka, S. Ito and A. Kishida, *J. Mater. Sci. Lett.*, 2003, **22**, 1737–40.
10. J. E. Mark, *Prog. Polym. Sci.*, 2003, **28**, 1205–21.
11. C. Sanchez and F. Ribot, *New J. Chem.*, 1994, **18**, 1007–47.
12. C. J. Brinker and G. W. Scherer, *Sol–Gel Science. The Physics and Chemistry of Sol–Gel Processing*, Academic Press, San Diego, CA, 1990.
13. N. Huesing and U. Schubert, *Synthesis of Inorganic Materials*, Wiley-VCH, Weinheim, 2004.
14. U. Schubert, *J. Mater. Chem.*, 2005, **15**, 3701–15.
15. G. Kickelbick and U. Schubert, *Monatsh. Chem.*, 2001, **132**, 13–30.
16. C. Sanchez, B. Lebeau, F. Ribot and M. In, *J. Sol-Gel Sci. Technol.*, 2000, **19**, 31–38.
17. Y. Abe and T. Gunji, *Prog. Polym. Sci.*, 2004, **29**, 149–82.
18. J. E. Mark, *Acc. Chem. Res.*, 2004, **37**, 946–53.
19. C. Guermeur, J. Lambard, J.-F. Gerard and C. Sanchez, *J. Mater. Chem.*, 1999, **9**, 769–78.
20. M. Nakade, K. Ichihashi and M. Ogawa, *J. Porous Mater.*, 2005, **12**, 79–85.
21. M. Nakade, K. Ichihashi and M. Ogawa, *J. Sol–Gel Sci. Technol.*, 2005, **36**, 257–64.
22. M. Nakade, K. Kameyama and M. Ogawa, *J. Mater. Sci.*, 2004, **39**, 4131–37.
23. B. Julian, C. Gervais, E. Cordoncillo, P. Escribano, F. Babonneau and C. Sanchez, *Chem. Mater.*, 2003, **15**, 3026–34.
24. B. Julian, C. Gervais, M.-N. Rager, J. Maquet, E. Cordoncillo, P. Escribano, F. Babonneau and C. Sanchez, *Chem. Mater.*, 2004, **16**, 521–29.
25. G. Kickelbick, J. Bauer, N. Huesing, M. Andersson and K. Holmberg, *Langmuir*, 2003, **19**, 10073–76.
26. G. Kickelbick, J. Bauer, N. Huesing, M. Andersson and A. Palmqvist, *Langmuir*, 2003, **19**, 3198–201.
27. G. J. d. A. A. Soler-Illia, E. L. Crepaldi, D. Grosso and C. Sanchez, *Curr. Opin. Colloid Interface Sci.*, 2003, **8**, 109–26.
28. D. Zhao, Q. Huo, J. Feng, B. F. Chmelka and G. D. Stucky, *J. Am. Chem. Soc.*, 1998, **120**, 6024–36.
29. R. C. Hayward, B. F. Chmelka and E. J. Kramer, *Adv. Mater. (Weinheim, Germany)*, 2005, vol. 17, pp. 2591–95.
30. H. Zhu, Z. Pan, B. Chen, B. Lee, S. M. Mahurin, S. H. Overbury and S. Dai, *J. Phys. Chem. B*, 2004, **108**, 20038–44.
31. Y. Chen, J. Du, M. Xiong, K. Zhang and H. Zhu, *Macromol. Rapid Commun.*, 2006, **27**, 741–50.
32. A. H. Yuwono, Y. Zhang, J. Wang, X. H. Zhang, H. Fan and W. Ji, *Chem. Mater.*, 2006, **18**, 5876–89.
33. L. C. Cauro-Gamet, L. G. Hubert-Pfalzgraf and S. Lecocq, *Z. Anorg. Allg. Chem.*, 2004, **630**, 2071–77.
34. S. Ivanovici, M. Puchberger, H. Fric and G. Kickelbick, *Monatsh. Chem.*, 2007, **138**, 529–39.
35. A. Kayan, D. Hoebbel and H. Schmidt, *J. Appl. Polym. Sci.*, 2005, **95**, 790–96.
36. J. N. Lee, C. Park and G. M. Whitesides, *Anal. Chem.*, 2003, **75**, 6544–54.
37. E. Favre, *Eur. Polym. J.*, 1996, **32**, 1183–88.
38. D. Hoebbel, T. Reinert, H. Schmidt and E. Arpac, *J. Sol–Gel Sci. Technol.*, 1997, **10**, 115–26.
39. C. Zhang and R. M. Laine, *J. Am. Chem. Soc.*, 2000, **122**, 6979–88.
40. B.-H. Kim, M.-S. Cho and H.-G. Woo, *Synlett*, 2004, 761–72.

